How to cite: *Angew. Chem. Int. Ed.* **2021**, *60*, 24075–24079
International Edition: doi.org/10.1002/anie.202103955
German Edition: doi.org/10.1002/ange.202103955

Protein NMR Spectroscopy

Pore-Bound Water at the Key Residue Histidine 37 in Influenza A M2

*Kumar Tekwani Movellan, Rıza Dervişoğlu, Stefan Becker, and Loren B. Andreas**

Abstract: *Atomic details of structured water molecules are indispensable to understand the thermodynamics of important biological processes including the proton conduction mechanism of the M2 protein. Despite the expectation of structured water molecules based on crystal structures of Influenza A M2, only two water populations have been observed by NMR in reconstituted lipid bilayer samples. These are the bulk- and lipid-associated water populations typically seen in membrane samples. Here, we detect a bound water molecule at a chemical shift of 11 ppm, located near the functional histidine 37 residue in the M2 conductance domain, which comprises residues 18 to 60. Combining 100 kHz magic-angle spinning NMR, dynamic nuclear polarization and density functional theory calculations, we show that the bound water forms a hydrogen bond to the δ1 nitrogen of histidine 37.*

The homo-tetrameric membrane protein Matrix 2 (M2) from Influenza A is a key protein in the viral life cycle. Although amantadine and rimantadine have long been used as first-line treatments against Influenza infection, resistant variants of the M2 protein prevent their use for currently circulating strains.[1] M2 is a pH-dependent proton channel that, in endosomes, acidifies the viral interior and thus triggers membrane fusion and viral RNA release into the host.[2] M2 proton conduction is also essential for preventing premature maturation of hemagglutinin by maintaining a high pH in the Golgi.[3]

The proton conduction mechanism has been studied in-depth by the combination of multiple techniques including biochemical[4] methods and high-resolution structural techniques.[5] Biochemical and electrophysiological data showed that the conserved residues histidine 37 (H37) and tryptophan 41 (W41) are responsible for proton selectivity and gating of M2, respectively.[4,6] While in M2 crystals the imidazole of H37 has been found in a box-like conformation with 4-fold symmetry,[5a,7] a dimer of dimers (C_2 symmetry) has been observed by magic-angle spinning (MAS) NMR for lipid bilayer preparations of the conductance domain (CD), which comprises approximately residue 18 to 60.[8] The resulting doubling of the NMR resonances, here indexed as A and B, was also observed for the full-length protein.[9] MAS NMR has also been used to investigate the pK_a of H37[10] and together with molecular dynamics simulation[11] there is a general agreement that the +3 charge state of H37 is the conductive state of the channel at the endosomal pH of ≤ 6.[12]

Both crystal and lipid bilayer conditions show a hydrated pore.[5d,13] Based on these data, proton diffusion via the Grotthuss mechanism[5c] is understood to occur in the pore outside the region of H37 and W41, which further restrict the pore volume. NMR data indicate a proton shuttle mechanism at residue H37.[14] In line with this, high-resolution X-Ray and XFEL data show organized water clusters in the pore of the transmembrane (TM) domain of M2 that adapt to a pH change.[5c] At low pH (< 5.5) the nearest water molecules are within hydrogen bonding distance to H37, and at high pH (8) the water cluster is far from the H37 imidazole. Drug binding causes structural changes in the protein[15] and disrupts the pore water network that is essential for proton conduction.[16]

In contrast to the multiple water locations identified in M2 crystals, NMR studies have only detected two water resonances in membrane-reconstituted M2 samples, namely bulk water at about 4.7 ppm and membrane-associated water (H_2O_{asd}) approximately 0.1 ppm downfield.[10b,17] Both represent an averaging of the chemical shift among many states in a pool of many water molecules in fast exchange. While long-lived water states with at least nanosecond residence times have been detected in soluble proteins,[18] observing the chemical shift of the bound-state water would require a longer residence time of at least milliseconds (ms).

While water molecules can be identified in very high-resolution crystal structures, the use of detergent for membrane proteins raises the possibility that such structures are perturbed from physiologically relevant conditions. For M2, the XFEL structures that resolved water clusters in the lumen of the TM protein[5c] do not capture the hydrogen bonding among H37 residues that is observed for the CD in lipids.[19] This indicates that the protein crystals have stabilized a different conformation than found for the CD in bilayers.

In CD M2, the H37 dimer-of-dimers chemical shifts have been assigned based on short (approx. 500 μs for ^{1}H to ^{15}N) cross polarization (CP) steps, in which transfer occurs primarily over a distance of a single chemical bond.[19a] Both A and B H37 residues are found in the τ tautomer.[19a,20] The deprotonated Nδ1 of $H37_A$ is hydrogen bonded to Hε2 of $H37_B$, but the hydrogen bonding partner of Nδ1 of $H37_B$ is not known. In TM M2, water is hydrogen bonded to Nδ1.[17a]

To probe for protons near the deprotonated Nδ1 of $H37_B$ (249 ppm),[19a] we acquired an (H)NH spectrum of CD M2 using long, 4 ms CP, and observed a proton correlation at approximately 11 ppm (Figure 1 A). This shift is partly

[*] Dr. K. T. Movellan, Dr. R. Dervişoğlu, Dr. S. Becker, Dr. L. B. Andreas
NMR based Structural Biology
Max Planck Institute for biophysical Chemistry
Am Fassberg 11, Göttingen 37077 (Germany)
E-mail: land@nmr.mpibpc.mpg.de

Supporting information and the ORCID identification number(s) for the author(s) of this article can be found under: https://doi.org/10.1002/anie.202103955.

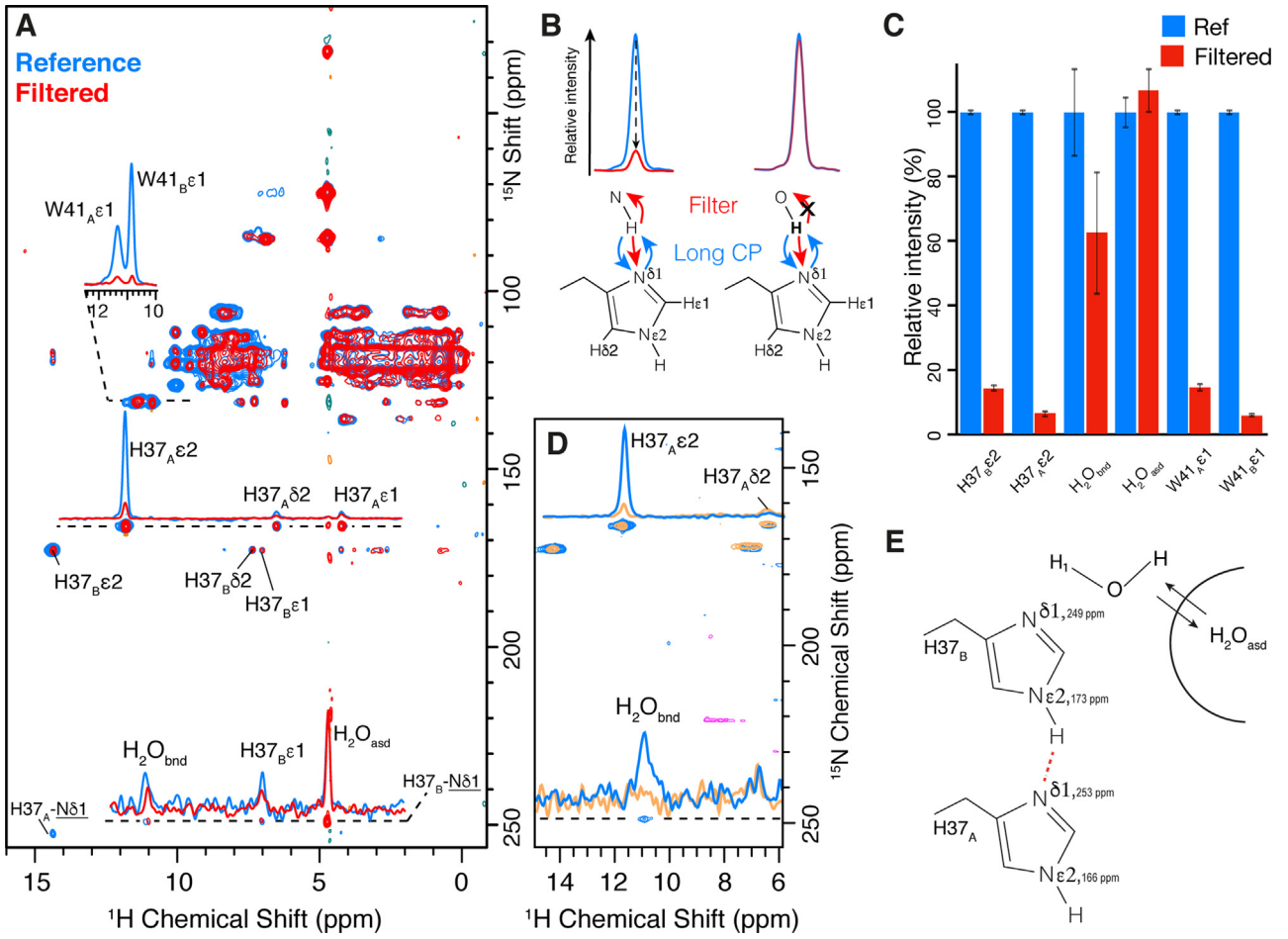

Figure 1. Identification of pore-bound water (H_2O_{bnd}). A) 2D (H)NH spectra with (red) and without (blue) a CP-based dipolar filter of 500 µs and 200 µs for ^{15}N and ^{13}C, respectively. Negative contours are green and orange. Additionally, in (A), 1D slices are shown at the selected H37 side-chain nitrogen resonances. B) Schematic representation of the expected signal intensity for the CP-based dipolar filtered spectrum of an amide (left) or water (right). For directly ^{15}N-bound amide protons the decay is fast. For water at a greater distance to nitrogen, the decay is slow such that the signal is marginally if at all reduced. C) Normalized peak intensities from CP-filtered spectra are plotted with error bars indicated at 2 times the variance, assuming gaussian-distributed spectrum noise. Bulk and bound water have a marginal reduction in the filtered experiment, while all ^{15}N-bound protons are below 20% of their signal. D) 2D (H)NH spectra of H_2O (blue) and D_2O-washed (orange) samples. Negative contours from the H_2O spectrum are pink. Unless indicated by an underline, labels indicate proton shifts. E) Schematic representation of the data showing the H_2O_{bnd} in ms exchange with H_2O_{asd}. Spectra of panel (A) were recorded with a 0.7 mm HCDN Bruker probe with 100 kHz MAS on a 950 MHz Bruker spectrometer at ca. 10°C (260 K cooling gas). CP transfer times of 4 ms were used. Twice the signal averaging was used for the filtered spectrum. The spectra of panel (B) were recorded on a 1.3 mm HCN Bruker probe with 45 kHz MAS on an 800 MHz Bruker spectrometer using 235 K cooling gas to reach a sample temperature below 10°C. Spectra were processed using a cosine squared apodization function, and for panel (B) also water gaussian suppression, "qfil".

overlapped with a W41 ε1 proton, but does not match any H^C or H^N peaks that appear in CP spectra, suggesting assignment to a bound water molecule (H_2O_{bnd}) in close proximity to $N\delta1_B$. Two other resonances correlate to $N\delta1_B$ in the CP spectrum, namely an H37 ε1 H^C at 7 ppm, and associated water at 4.8 ppm. There is precedence for a resonance far from the bulk water chemical shift of 4.7 ppm in the form of a 19 ppm water proton of a synthetic carbonic anhydrase complex.[21]

To confirm the assignment, we applied a CP-based dipolar filter to exclude H^N protons (Figure 1 A, S1).[22] The dipolar filter causes protons that are bonded to ^{15}N or ^{13}C to lose intensity faster than those that are more distant, as shown schematically in Figure 1 B. The ^{15}N filter is important since the 11 ppm peak partly overlaps with a W41 indole proton. There are no overlapping peaks in the (H)CH spectrum (Figure S2). The indole proton intensities are efficiently filtered, while the water proton intensity decreases more slowly, consistent with the longer distance in a hydrogen bond (Figure 1 A,C). Similar dipolar filtering of H^C protons was less efficient. We therefore exchanged the supernatant of the membrane pellet with buffer containing 99% D_2O and recorded another (H)NH spectrum after 48 hours (Figure S3). Loss of the H_2O_{bnd} intensity confirms that the proton is exchangeable, and not bonded to ^{13}C. By comparison, the δ2 and ε1 H^C peaks at 6–7 ppm retain full intensity (Figure 1 B and Figure S3). There are three side chains with exchangeable protons in the M2 transmembrane pore, S31,

H37, and W41. Imidazole and indole H^N protons have been assigned previously (Figure S4).[19a] The CP-filtered spectrum excludes them as an assignment possibility. S31 lies about two helical turns from H37, too distant for CP transfer. Water is then the only remaining assignment possibility. The arrangement of H_2O_{bnd} and H_2O_{asd} is shown schematically in Figure 1E with the 11 ppm water proton labeled H_1.

To quench potential water dynamics and exchange,[23] we recorded similar proton-detected NH correlation spectra at 90 K using DNP. For these measurements we mutated the only other histidine, H57, to tyrosine, to avoid any spectral overlap with the H37 peaks of interest. Using TEMTriPOL[24] and a four-channel Phoenix probe at 24 kHz MAS, we obtained a DNP enhancement factor, ε, of 22, measured from carbon CP spectra. To determine the effective pH in the frozen sample, we used a color indicator,[25] and noted a small drop in pH from 7.8 to 7 (Figure S5), where the channel is still predominantly neutral; this is well above a pH of 6.2 where the +2 charge state is maximized, with hydrogen bonded H37 residues.[19b] The relatively fast MAS of 24 kHz results in resolved side chain protons, and the bound water can be observed in contact with the imidazole at the same chemical shift of 11 ppm that was present at 283 K (Figure 2A and Figure S6). At 100 K, the dipolar filtered spectrum again highlights the H_2O_{bnd} signal, which retains circa 50% intensity, compared with 25% for histidine side chain protons (Figure 2B and Figure S6).

Since both 10 °C and cryogenic temperatures resulted in the same H_2O_{bnd} chemical shift, these data indicate that the H_2O_{bnd} is not averaged via exchange, but represents a single bound water molecule. This is consistent with the slow conversion of the circa 11 ppm peak to the H_2O_{asd} chemical shift, which occurs over several ms at 10 °C, as can be observed in the long CP spectrum. It suggests that the bound water forms a hydrogen bond that is stable for milliseconds even at room temperature.

To extend our understanding of the water binding geometry near Nδ1 of $H37_B$, we performed density functional theory (DFT)-based calculations of NMR chemical shifts starting from an experimental MAS NMR structure (details in the Supporting Information) in which a water molecule was placed near Nδ1 of $H37_B$. Chemical shift information is sensitive to the local atomic environment and in particular to hydrogen bonding.[26] Two starting structures were considered during the geometry optimization, either a tetramer or a dimer spanning from residue G34 to W41. For faster convergence, the tetramer was further split into two dimers for the NMR calculation. Depending on the starting structure for DFT optimization, the water molecule is found in two different positions after optimization (Figure S7 and S8), both with a first proton forming a 1.6 Å hydrogen bond to Nδ1 of $H37_B$. In one, the second proton is facing the pore (Figure 3A and Figure S7A) and in the other it is bridging to the backbone amide nitrogen of G34 (Figure S8). The basis set 6-311++g(d,p) improves the agreement to experimental data for the isotropic chemical shifts to within 3 and 8 ppm for ^1H and ^{15}N, respectively (Figure S7 and S8). The largest deviations in nitrogen shifts are found for Nε2 and Hε2 of $H37_A$ where limited structural restraints are available from the NMR data. On the other hand, the calculated shift of 13.97 ppm is close to the experimental value of 14.27 ppm for the proton that forms the imidazole–imidazole hydrogen bond.

In nearly perfect agreement with the experimental water proton chemical shift (δH_{exp}) of approx. 11 ppm, the calculated proton chemical shift (δH_{calc}) is found at 10.7 ppm for the case of bridging water. For $N\delta1_B$, δN_{exp} of 249 ppm also agrees with $\delta N_{calc} \approx 248.2$ ppm for this structure (Figure S8D). For the case of pore facing water, $\delta N_{calc} \approx 249.0$ ppm, match-

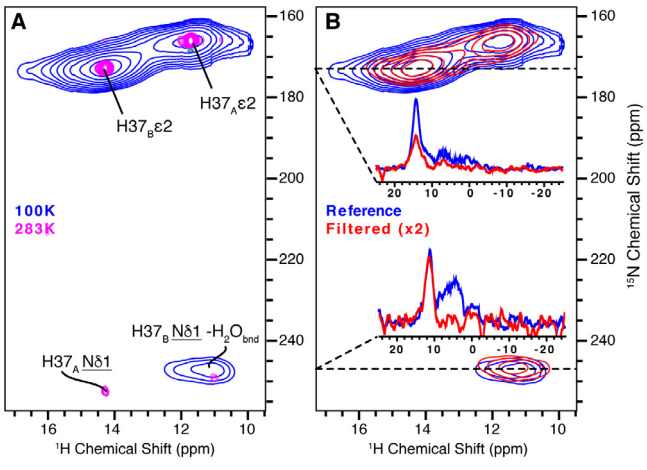

Figure 2. Water detected near the H37 imidazole using DNP. A) Overlay of the 2D (H)NH spectrum at 283 K (pink) and DNP at 100 K (blue). B) 100 K (H)NH water-edited DNP spectra (24 kHz MAS) without CP filter (blue) and with a 200 µs CP filter (red). The DNP spectra are of M2 H57Y at pH ≈ 7 using 3 ms CP transfers. The insets show the 1D proton slices of the $H37_B$ Nε2, as well as Nδ1, which is correlated with the proton H_2O_{bnd}.

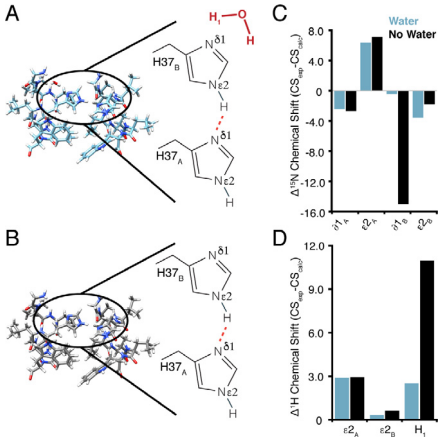

Figure 3. Chemical shifts of the M2 pore water calculated by DFT using the 6-311++g(d,p) basis set with the B3LYP level of theory. The dimer structures used as input for the calculation are shown A) with and B) without the presence of a water molecule. In both, residue G34 to W41 of the tetramer structure obtained from an experimental NMR structure calculated with CYANA was geometry-optimized with DFT (see SI Table 1 for the assignments and restraints used for CYANA calculation of the NMR structure). Comparison of calculated and experimental chemical shifts with (blue) or without water (black) are shown for C) nitrogen and D) proton.

ing δN_{exp}, but δH_{calc} is 8.5 ppm, which deviates about 2.5 ppm (Figure 3D) from the δH_{exp}. The better match for bridging water suggests that the bound water molecule establishes hydrogen bonds for both protons. Including additional solvation in the calculation by using the polarizable continuum model (CPCM solvent = H2O)[27] did not substantially change the result (Figure S7).

An identical calculation without water (Figure 3B) resulted in a δN_{calc} for Nδ1 of $H37_B$ that differs by 15 ppm from the δN_{exp} (Figure 3C). In contrast, the chemical shifts for Hε2 and Nε2, which are farther from the water location, are not affected by removal of water (Figure 3C,D). In both bridging and pore-facing cases, an agreement emerges that a water molecule is hydrogen bonded to the deprotonated nitrogen of the histidine imidazole at high pH, pH 7 to 7.8.

In summary, the combined NMR and DFT data indicate that at high pH (> 7) and in the presence of the imidazole–imidazole hydrogen bond there is hydrogen-bonded water at $N\delta1_B$ of the pH-sensing residue H37 of M2. This is contrary to crystallographic data where the water molecules are close enough to form a hydrogen bond only at low pH.[5c] The investigation of other water molecules in the pore, and how they relate to conformations trapped in protein crystals, was not possible since, without freezing the sample, such water molecules are likely indistinguishable from membrane-associated water by chemical shift. Detecting additional water molecules may be possible in the future by a combination of faster MAS and cryogenic temperatures.

The combination of fast MAS, which narrows resonances, D_2O exchange, and dipolar filtering to select against protein signals, overcomes the challenge of identifying water protons. The result is identification of a bound water at 11 ppm in membrane-embedded M2. Since water displacement is a significant contribution to the binding thermodynamics, the detailed water structure will inform future drug development efforts.

Acknowledgements

We thank Melanie Wegstroth and Kerstin Overkamp for the sample preparation, Dr. Andrei Leonov for support of protein sample preparation, Dr. Juan Carlos Fuentes-Monteverde for discussing DFT, and Marcel Forster and Vrinda Sant for critically reading the manuscript. We thank J. Schimpfhauser and J. Bienert at Dr. V. N. Belov's Laboratory at Max Planck Institute for Biophysical Chemistry, Göttingen for synthesizing the TEMTriPol-1 radical. Funding is acknowledged from DFG grant AN1316/1-1. Open Access funding enabled and organized by Projekt DEAL.

Conflict of Interest

The authors declare no conflict of interest.

Keywords: dynamic nuclear polarization · hydrogen bonding · pore-bound water · proton conduction · solid-state NMR

[1] G. Dong, C. Peng, J. Luo, C. Wang, L. Han, B. Wu, G. Ji, H. He, *PLoS One* **2015**, *10*, e0119115.
[2] a) T. Sakaguchi, Q. Tu, L. H. Pinto, R. A. Lamb, *Proc. Natl. Acad. Sci. USA* **1997**, *94*, 5000–5005; b) C. Wang, K. Takeuchi, L. H. Pinto, R. A. Lamb, *J. Virol.* **1993**, *67*, 5585–5594; c) L. H. Pinto, L. J. Holsinger, R. A. Lamb, *Cell* **1992**, *69*, 517–528; d) L. J. Holsinger, D. Nichani, L. H. Pinto, R. A. Lamb, *J. Virol.* **1994**, *68*, 1551–1563.
[3] T. Sakaguchi, G. P. Leser, R. A. Lamb, *J. Cell Biol.* **1996**, *133*, 733–747.
[4] C. Wang, R. A. Lamb, L. H. Pinto, *Biophys. J.* **1995**, *69*, 1363–1371.
[5] a) R. Acharya, V. Carnevale, G. Fiorin, B. G. Levine, A. L. Polishchuk, V. Balannik, I. Samish, R. A. Lamb, L. H. Pinto, W. F. DeGrado, M. L. Klein, *Proc. Natl. Acad. Sci. USA* **2010**, *107*, 15075–15080; b) S. D. Cady, K. Schmidt-Rohr, J. Wang, C. S. Soto, W. F. Degrado, M. Hong, *Nature* **2010**, *463*, 689–692; c) J. L. Thomaston, R. A. Woldeyes, T. Nakane, A. Yamashita, T. Tanaka, K. Koiwai, A. S. Brewster, B. A. Barad, Y. Chen, T. Lemmin, M. Uervirojnangkoorn, T. Arima, J. Kobayashi, T. Masuda, M. Suzuki, M. Sugahara, N. K. Sauter, R. Tanaka, O. Nureki, K. Tono, Y. Joti, E. Nango, S. Iwata, F. Yumoto, J. S. Fraser, W. F. DeGrado, *Proc. Natl. Acad. Sci. USA* **2017**, *114*, 13357–13362; d) J. L. Thomaston, M. Alfonso-Prieto, R. A. Woldeyes, J. S. Fraser, M. L. Klein, G. Fiorin, W. F. DeGrado, *Proc. Natl. Acad. Sci. USA* **2015**, *112*, 14260–14265.
[6] Y. Tang, F. Zaitseva, R. A. Lamb, L. H. Pinto, *J. Biol. Chem.* **2002**, *277*, 39880–39886.
[7] A. L. Stouffer, R. Acharya, D. Salom, A. S. Levine, L. Di Costanzo, C. S. Soto, V. Tereshko, V. Nanda, S. Stayrook, W. F. DeGrado, *Nature* **2008**, *451*, 596–599.
[8] M. Sharma, M. Yi, H. Dong, H. Qin, E. Peterson, D. D. Busath, H. X. Zhou, T. A. Cross, *Science* **2010**, *330*, 509–512.
[9] Y. Miao, H. Qin, R. Fu, M. Sharma, T. V. Can, I. Hung, S. Luca, P. L. Gor′kov, W. W. Brey, T. A. Cross, *Angew. Chem. Int. Ed.* **2012**, *51*, 8383–8386; *Angew. Chem.* **2012**, *124*, 8508–8511.
[10] a) M. T. Colvin, L. B. Andreas, J. J. Chou, R. G. Griffin, *Biochemistry* **2014**, *53*, 5987–5994; b) S. Li, M. Hong, *J. Am. Chem. Soc.* **2011**, *133*, 1534–1544.
[11] a) I. Kass, I. T. Arkin, *Structure* **2005**, *13*, 1789–1798; b) R. Liang, J. M. J. Swanson, J. J. Madsen, M. Hong, W. F. DeGrado, G. A. Voth, *Proc. Natl. Acad. Sci. USA* **2016**, *113*, E6955–E6964.
[12] J. Hu, R. Fu, K. Nishimura, L. Zhang, H. X. Zhou, D. D. Busath, V. Vijayvergiya, T. A. Cross, *Proc. Natl. Acad. Sci. USA* **2006**, *103*, 6865–6870.
[13] C. Tian, P. F. Gao, L. H. Pinto, R. A. Lamb, T. A. Cross, *Protein Sci.* **2003**, *12*, 2597–2605.
[14] a) C. Wei, A. Pohorille, *Biophys. J.* **2013**, *105*, 2036–2045; b) F. Hu, K. Schmidt-Rohr, M. Hong, *J. Am. Chem. Soc.* **2012**, *134*, 3703–3713.
[15] a) L. B. Andreas, M. T. Eddy, R. M. Pielak, J. Chou, R. G. Griffin, *J. Am. Chem. Soc.* **2010**, *132*, 10958–10960; b) S. D. Cady, W. Luo, F. Hu, M. Hong, *Biochemistry* **2009**, *48*, 7356–7364.
[16] J. L. Thomaston, N. F. Polizzi, A. Konstantinidi, J. Wang, A. Kolocouris, W. F. DeGrado, *J. Am. Chem. Soc.* **2018**, *140*, 15219–15226.
[17] a) M. Hong, K. J. Fritzsching, J. K. Williams, *J. Am. Chem. Soc.* **2012**, *134*, 14753–14755; b) C. Shi, C. Oster, C. Bohg, L. Li, S. Lange, V. Chevelkov, A. Lange, *J. Am. Chem. Soc.* **2019**, *141*, 17314–17321.
[18] J. Qvist, G. Ortega, X. Tadeo, O. Millet, B. Halle, *J. Phys. Chem. B* **2012**, *116*, 3436–3444.
[19] a) K. T. Movellan, M. Wegstroth, K. Overkamp, A. Leonov, S. Becker, L. B. Andreas, *J. Am. Chem. Soc.* **2020**, *142*, 2704–2708;

b) R. Fu, Y. Miao, H. Qin, T. A. Cross, *J. Am. Chem. Soc.* **2020**, *142*, 2115 – 2119.
[20] L. B. Andreas, M. Reese, M. T. Eddy, V. Gelev, Q. Z. Ni, E. A. Miller, L. Emsley, G. Pintacuda, J. J. Chou, R. G. Griffin, *J. Am. Chem. Soc.* **2015**, *137*, 14877 – 14886.
[21] S. B. Lesnichin, I. G. Shenderovich, T. Muljati, D. Silverman, H. H. Limbach, *J. Am. Chem. Soc.* **2011**, *133*, 11331 – 11338.
[22] X. L. Wu, K. W. Zilm, *J. Magn. Reson. Ser. A* **1993**, *102*, 205 – 213.
[23] J. R. Long, R. Ebelhäuser, R. G. Griffin, *J. Phys. Chem. A* **1997**, *101*, 988 – 994.
[24] G. Mathies, M. A. Caporini, V. K. Michaelis, Y. Liu, K. N. Hu, D. Mance, J. L. Zweier, M. Rosay, M. Baldus, R. G. Griffin, *Angew. Chem. Int. Ed.* **2015**, *54*, 11770 – 11774; *Angew. Chem.* **2015**, *127*, 11936 – 11940.
[25] a) G. Gómez, M. J. Pikal, N. Rodriguez-Hornedo, *Pharm. Res.* **2001**, *18*, 90 – 97; b) D. L. Williams-Smith, R. C. Bray, M. J. Barber, A. D. Tsopanakis, S. P. Vincent, *Biochem. J.* **1977**, *167*, 593 – 600.
[26] E. Y. Tupikina, M. Sigalov, I. G. Shenderovich, V. V. Mulloyarova, G. S. Denisov, P. M. Tolstoy, *J. Chem. Phys.* **2019**, *150*, 114305.
[27] J. L. Pascual-Ahuir, E. Silla, J. Tomasi, R. Bonaccorsi, *J. Comput. Chem.* **1987**, *8*, 778 – 787.

Manuscript received: March 19, 2021
Revised manuscript received: August 2, 2021
Accepted manuscript online: September 3, 2021
Version of record online: October 6, 2021

